



Synthesis of modified polyepoxysuccinic acid and evaluation of its scale inhibition on CaCO_3 , CaSO_4 and $\text{Ca}_3(\text{PO}_4)_2$ precipitation for industrial recycling water

Yiyi Chen^a, Yuming Zhou^{a,b,*}, Qingzhao Yao^{b,*}, Qiuli Nan^b, Mingjue Zhang^b, Wei Sun^c

^aSchool of Chemistry and Chemical Engineering, Southeast University, Nanjing 211189, China, Tel. +86 25 52090617; email: chenyyiyi0220@126.com

^bDepartment of Chemical and Pharmaceutical Engineering, Southeast University Chengxian College, Nanjing 210032, China, Tel. +86 25 52090617; emails: ymzhou@seu.edu.cn (Y. Zhou), 101006377@seu.edu.cn (Q. Yao), 53212651@qq.com (Q. Nan), 489354839@qq.com (M. Zhang)

^cJianghai Environmental Protection Co., Ltd., Changzhou 213116, China, Tel. +86 25 52090617; email: leojhhg@sina.com

Received 10 September 2018; Accepted 3 February 2019

ABSTRACT

Modified polyepoxysuccinic acid (PESA) scale inhibitor, ESA-co-APEM (PEM), was prepared through free-radical polymerization on PESA with oxalic acid-allylpolyethoxy carboxylate, and then applied for the inhibition of calcium scales from cooling water, such as CaCO_3 , CaSO_4 and $\text{Ca}_3(\text{PO}_4)_2$. The structure of PEM was characterized by Fourier transform infrared (FTIR), ^1H NMR, and ^{13}C NMR, and the inhibition performance toward CaCO_3 , CaSO_4 and $\text{Ca}_3(\text{PO}_4)_2$ was studied by the method of static scale inhibition test with different dosages. The polymer PEM exhibited more excellent scale inhibition property against calcium scales than PESA and the comprehensive scale inhibition property of PEM was much better than the property of PESA. The maximum CaCO_3 efficiency of PEM was as high as 94.5% in the concentration of 12 mg/L, while at a level of 4 mg/L PEM, the inhibition efficiency of CaSO_4 reached 98.2%. Moreover, PEM had an efficiency of 99.5% for $\text{Ca}_3(\text{PO}_4)_2$ at a level of 8 mg/L. The modified calcium scales in the presence of PEM were analyzed by scanning electron microscopy, X-ray powder diffraction, and transmission electron microscopy, respectively.

Keywords: Polyepoxysuccinic acid; Modification; Calcium carbonate; Calcium sulfate; Calcium phosphate; Mechanism

1. Introduction

The natural water employed in industrial cooling systems often contains a large number of dissolved salts of calcium ions. With cycled use of cooling water, calcium ions in the water become concentrated and form insoluble salts, which can cause scale deposit on the surface of heat transfer apparatus, bringing about low heat transfer efficiency, reduced cooling effect, and corrosion of metal equipment. Three commonly available calcium scales are calcium carbonate, calcium sulfate, and calcium phosphate [1–4]. An effective method for

controlling scale formation in circulating cooling water system is the use of scale inhibitors. The noticeable advantage of this scale inhibition technique is that, when properly applied, an inhibitor can repress scale formation at very low dosage and hence, at an affordable cost [5,6].

Biodegradable polymers, such as polyaspartic acid and polyepoxysuccinic acid (PESA), have drawn much attention recently in view of environmental benefits. In particular, PESA is a circulating water scale inhibitor with double features of scale inhibition and dispersion, and it

* Corresponding authors.

is a representative among green scale inhibitors given its nontoxicity, good biodegradability with broad application prospect and environmental acceptability [7–9]. It is the non-phosphorus and nitrogen free “green” water treatment agent, and originally developed by the United States Co. Betz and Proctor & Gamble in the early 1990s of 20th century [10,11]. Many researchers have studied and discussed synthesis and multi-scale inhibition of PESA [12,13]. Shi et al. [3] have chosen itaconic acid (IA) and ESA as monomers to prepare environment friendly antiscalant, and PIA-co-ESA copolymer exhibits excellent scale inhibition performance. Zhou et al. [14] have evaluated the inhibition and dispersion of PESA and the experimental results demonstrated that PESA exhibited excellent scale inhibition to CaCO_3 and $\text{Ca}_3(\text{PO}_4)_2$, good stability to zinc salt, and special dispersion to ferric oxide. Nevertheless, as it only contains carboxylic group, the comprehensive scale inhibition performance of PESA is poor, which limits its use. In order to improve the performance, chemical modification, such as introducing new functional groups into the side chain of PESA, is proven to be available [15,16].

The carboxylic groups in the polymer are the main functional groups inhibiting the formation of calcium carbonate and calcium sulfate scales, the hydroxylic groups are the main functional groups inhibiting the formation of calcium phosphate, while ether groups exhibit good dispersion performance, which can effectively prevent the formation of chelate precipitation. Moreover, the polyethers in the molecule could increase the solubility of polymer in aqueous solutions, and the polyesters are easily biodegradable since the ester bonds can be hydrolyzed into carboxyl and hydroxyl groups [17–19]. In this study, a modified and new polyepoxysuccinic acid inhibitor was synthesized with epoxysuccinic acid and oxalic acid-allylpolyethoxy carboxylate as monomers, water as solvent and ammonium persulfate as initiator by the free-radical polymerization. Only containing carboxylic, hydroxylic, ether, and ester groups, PEM is environmental friendly as there are no phosphorus (P), nitrogen (N), and sulphur (S) in its molecular formula. The structure of PEM was identified by Fourier transform infrared (FTIR), $^1\text{H-NMR}$, and $^{13}\text{C-NMR}$, and the inhibiting efficiency toward CaCO_3 , CaSO_4 , and $\text{Ca}_3(\text{PO}_4)_2$ was studied by the method of

static scale inhibition test at different dosages. Moreover, the morphology of crystals was observed by scanning electron microscopy (SEM), X-ray powder diffraction (XRD), and transmission electron microscopy (TEM), respectively.

2. Experimental Setup

2.1. Materials

Maleic anhydride, hydrogen peroxide, sodium tungstate, calcium chloride, sodium bicarbonate, sodium sulfate, monopotassium phosphate, ammonium persulfate, and ascorbic acid used were obtained from Zhongdong Chemical Reagent Co., Ltd. (Nanjing, Jiangsu, People's Republic of China). All chemicals above were of analytical reagent grade and used without further purification. Distilled water was used throughout the experiments.

2.2. Synthesis of ESA, APEM, and PEM

The synthesis procedure of ESA is shown in Fig. 1. 9.8 g (0.1 mol) of maleic anhydride was dissolved in a three-neck flask under alkaline conditions and 20 mL of hydrogen peroxide was slowly added into it, and reacted at 50°C for 1.5 h with magnetic stirring. Then, the solution was separated with ethyl alcohol and dried under nitrogen to 90°C .

Synthesis procedure of APEM is shown in Fig. 2. APEM was synthesized in our laboratory according to our previous studies [20]. Allyloxy polyethoxy ether was carboxylate terminated using oxalic acid with a molar ratio of 1:1.

The synthesis procedure of PEM from ESA and APEM is shown in Fig. 3. ESA was copolymerized with APEM in aqueous medium. A 250-mL round-bottom flask equipped with a mechanical stirrer, thermometer, 0.05 mol APEM, and reflux condenser was charged with 30 mL DI water and a total of 0.1 mol ESA (the mole ratio of ESA to APEM was 2:1), then heated to the reaction temperature of 70°C over a period of time under nitrogen atmosphere. In mixed conditions, the initiator ammonium persulfate was dropped at a certain flow rate separately for about 1.5 h. Finally, the modified biodegradable polymer PEM was obtained, containing about 20.34% solid.

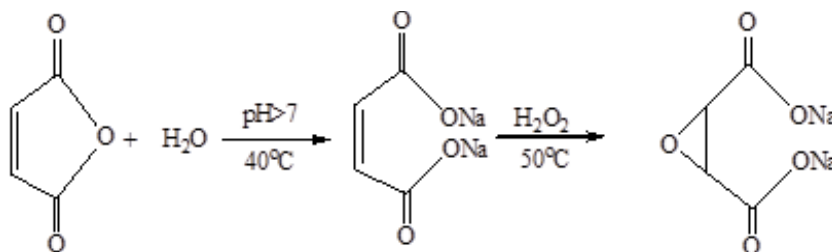


Fig. 1. Preparation of ESA.

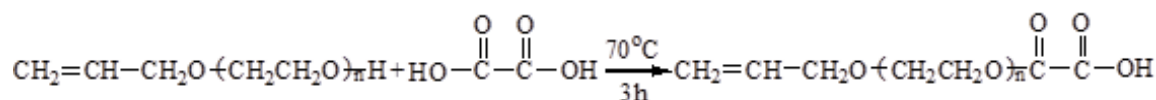


Fig. 2. Preparation of APEM.

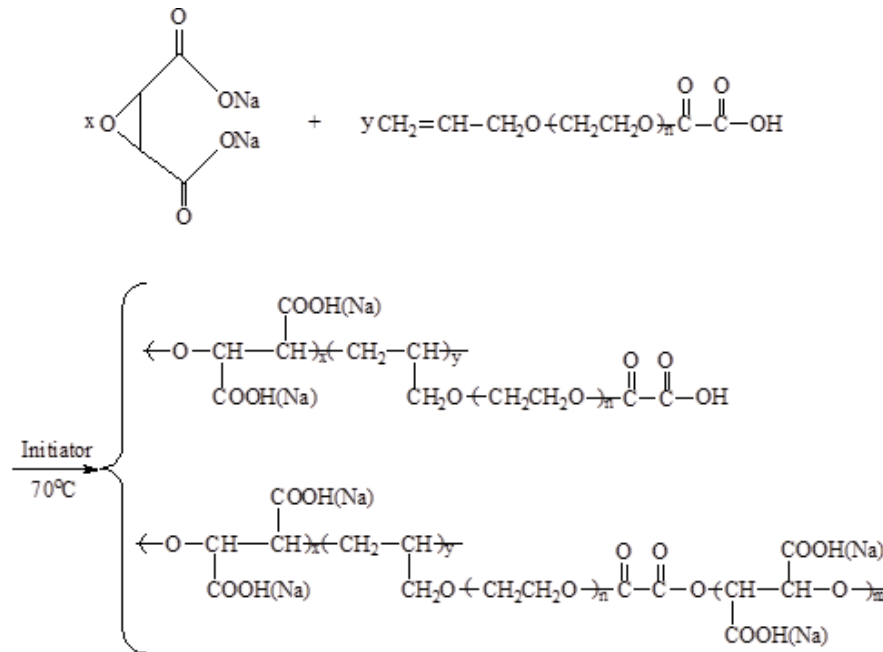


Fig. 3. Preparation of PEM.

2.3. Characterization of ESA, APEM, and PEM

Gel permeation chromatography (calibrated with PEG standards) was utilized to determine the molecular weight of PEM with water as the mobile phase at a flow rate of 1.0 mL/min. The stability of the polymer PEM was performed by thermogravimetric analysis (TGA) using a thermal gravimetric analysis apparatus at temperatures ranging from 0°C to 300°C. The structure of polymer was analyzed by FTIR spectroscopy (VECTOR-22, Bruker Co., Germany) between 4,500 and 0 cm^{-1} , which was used to confirm the presence of expected functional groups responsible for the scale inhibition property. About 1 mg dried PEM was mixed with 100 mg dried KBr powder and then compressed into a disk for spectrum recording. A Bruker NMR analyzer (AVANCE AV-500, Bruker, Switzerland) was also used to explore the structures of ESA, APEM, and PEM, operating at 500 MHz.

2.4. Inhibition performance against CaCO_3 scale

The prepared polymers estimated the scale inhibition performance against calcium carbonate by the static scale inhibition test referring to literature, the National Standard of the People's Republic of China (GB/T16632-2008) [21]. The initial test solution contained 240 mg/L Ca^{2+} (made by using CaCl_2) and 732 mg/L CO_3^{2-} (made by using NaHCO_3). The mixed solutions without or with different concentrations of PEM scale inhibitor were maintained at 80°C for 10 h, then they were cooled to room temperature. The Ca^{2+} concentrations of all of those solutions were titrated by 0.05 mg/L sodium ethylene diamine tetraacetate (EDTA) standard solution. The inhibition efficiency η was defined by Eq. (1):

$$\eta = \frac{\rho_1(\text{Ca}^{2+}) - \rho_2(\text{Ca}^{2+})}{\rho_0(\text{Ca}^{2+}) - \rho_2(\text{Ca}^{2+})} \times 100\% \quad (1)$$

where ρ_0 (Ca^{2+}) is the total concentrations of Ca^{2+} (mg/L), ρ_1 (Ca^{2+}) is the concentrations of Ca^{2+} (mg/L) in the presence of the polymer inhibitor, ρ_2 (Ca^{2+}) is the concentrations of Ca^{2+} (mg/L) in the absence of the polymer inhibitor.

2.5. Inhibition performance against CaSO_4 scale

The scale inhibition performance of the prepared polymer against calcium sulfate was investigated by static scale inhibition tests according to the Chinese National Standard concerning the Code for the Design of Industrial Oil Fieldwater Treatments (SY/T 5673-93) [22]. The solution in calcium sulfate inhibition tests contained CaCl_2 (6,800 mg/L Ca^{2+}), Na_2SO_4 (7,100 mg/L of SO_4^{2-}) and different concentration of polymers, which then was heated in a water bath at 60°C for 6 h and the determination of Ca^{2+} was done by exactly same process.

2.6. Inhibition performance against $\text{Ca}_3(\text{PO}_4)_2$ scale

In this experiment, the inhibition efficiency of PEM against calcium phosphate precipitation was determined according to the National Standard of China Concerning the Code for the Design of Industrial Circulating Cooling-Water Treatment (GB 50050-95) [23]. A known volume of phosphate stock solution (the final PO_4^{3-} concentration would be 5 mg/L) was added to a glass bottle (250 mL) with a known volume of water, while the inhibitors were added before the calcium stock solution was added in such amount that the final calcium concentration would be 250 mg/L or the required values. After these solutions were heated 10 h at a temperature of 80°C, precipitation in these solutions was monitored by analyzing aliquots of the filtered (0.22 μm) solution for phosphate concentration by using the standard colorimetric method according to the International Standard ISO 6878:2004 [24].

Investigation with and without inhibitors were all carried out. Anti-scalant efficiency as a calcium phosphate inhibitor was calculated by using the following equation:

$$\text{inhibition}(\%) = \frac{[\text{phosphate}]_{\text{final}} - [\text{phosphate}]_{\text{blank}}}{[\text{phosphate}]_{\text{initial}} - [\text{phosphate}]_{\text{blank}}} \times 100\% \quad (2)$$

where $[\text{phosphate}]_{\text{final}}$ = concentration of phosphate in the filtrate in the presence of inhibitors at 10 h, $[\text{phosphate}]_{\text{blank}}$ = concentration of phosphate in the filtrate in the absence of inhibitors at 10 h, and $[\text{phosphate}]_{\text{initial}}$ = concentration of phosphate at the beginning of the experiment.

2.7. Morphology characterization

The morphological changes of CaCO_3 was examined through SEM and XRD, CaSO_4 crystals through SEM and $\text{Ca}_3(\text{PO}_4)_2$ crystals through TEM, with the addition of the polymer. The samples were coated with a layer of gold and observed in a SEM (S-3400N, HITECH, Taiwan, China). A TEM (JEM-2100SX, Japan) was also used to observe the shape of calcium crystals.

3. Results and discussion

3.1. Characterization results of synthetic products

As an important parameter in the process of scale inhibition, the molecular weight has been detected. APEM's molecular weight was $320 \text{ g}\cdot\text{mol}^{-1}$, whereas PEM's number-average molecular weight (M_n) was $16.8 \times 10^3 \text{ g}\cdot\text{mol}^{-1}$ (ESA:APEM [2:1]).

TGA was used to investigate the thermal stability of PEM and the corresponding curve is displayed in Fig. 4. According to the curve, the degradation of PEM proceeded in two stages, among which the first part was the evaporation of some water in the polymer, about 80% weight loss. Then

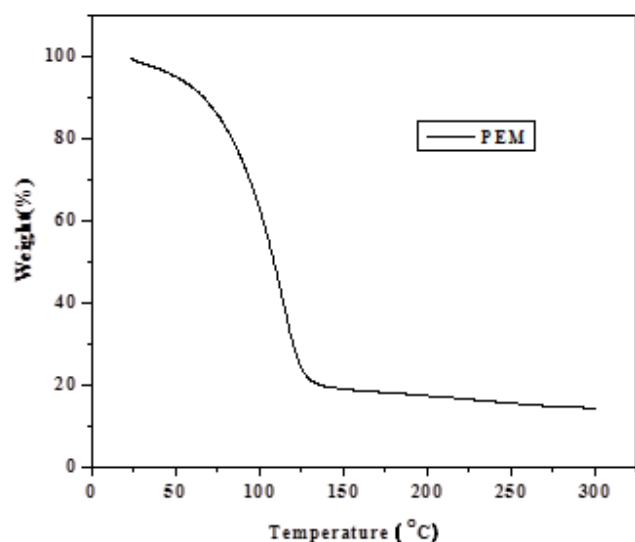


Fig. 4. TGA curve for PEM polymer.

the weight loss was less than 1% with temperature rising. Therefore, the stability of PEM was good enough.

In order to verify the structure of ESA, APEM, and PEM, IR curves are illustrated in Fig. 5. In IR spectrum (a), the absorption peak at 850 cm^{-1} is attributed to the deformation vibration of C–O–C (closed loop), the peak at 945 cm^{-1} is the symmetrical stretching vibration of C–O–C (closed loop), while the absorption peak of $1,230 \text{ cm}^{-1}$ is the asymmetric stretching vibration of C–O–C (closed loop). The above signals indicate the existence of a three-membered ring epoxy structure and reveal that the designed targeted functional groups had been introduced onto PESA backbones. Meanwhile, the peak at $1,314 \text{ cm}^{-1}$ is the bending vibration of C–H, the peak at $1,405 \text{ cm}^{-1}$ is in-plane bending vibration of O–H, the peak at $3,038 \text{ cm}^{-1}$ is the stretching vibration of C–H (methenyl), the peak at $3,348 \text{ cm}^{-1}$ is the stretching vibration of O–H, demonstrating that it is ESA [25–27].

On the other hand, the peak that appears at $1,650 \text{ cm}^{-1}$ in curve (b) is for the C=C stretching vibration, while there are no peaks between $1,620$ and $1,680 \text{ cm}^{-1}$ in curve (c).

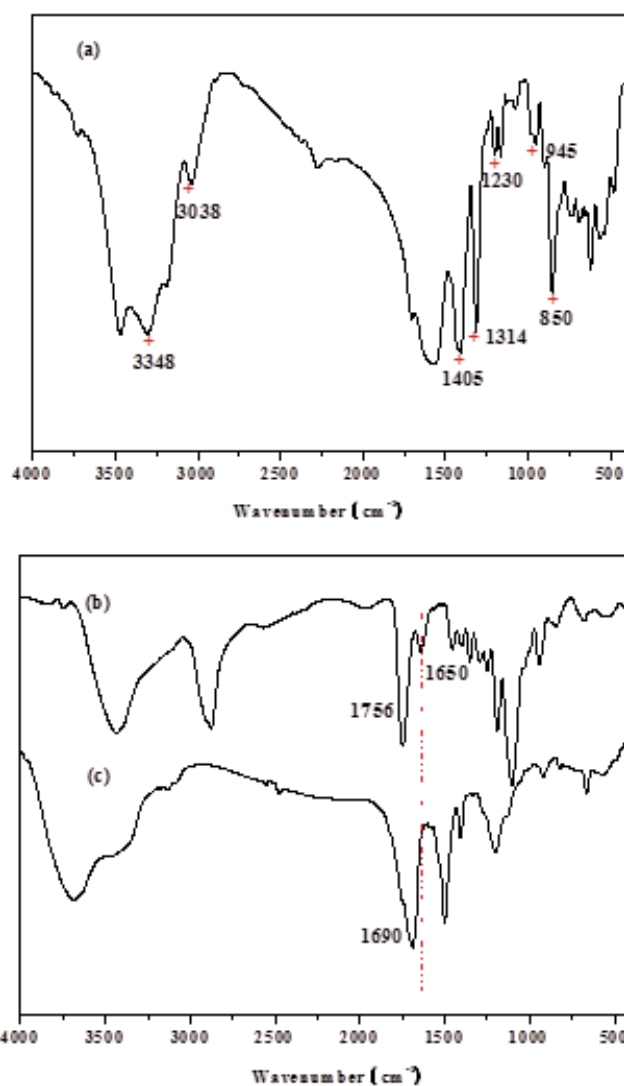


Fig. 5. FTIR spectra of ESA (a), APEM (b), and PEM (c).

Meanwhile, the absorption peaks at 3,038, 1,230, and 945 cm^{-1} also disappear and the absorption peak at 1,128 cm^{-1} is the stretching vibration of cycle C–O–C bond, indicating that PEM has been successfully synthesized. 1,756 and 1,690 cm^{-1} are absorption peaks of the ester bond in APEM and PEM molecules, respectively.

^{13}C NMR spectrum of ESA is displayed in Fig. 6, using $(\text{CD}_3)_2\text{SO}$ as solvent. It is seen that peaks between 37.390 and 38.659 ppm are the solvent residual peak of $(\text{CD}_3)_2\text{SO}$, 130.481 ppm is the signal of C=C of the residual maleic anhydride, and 173.362 and 175.147 ppm are assigned to C=O. Moreover, the peak at 55.268 ppm is attributed to C–O–C (closed loop), and there is no adsorption peak of C–C at 85.4 ppm. Therefore, it can be supposed that ESA was synthesized successfully and no by-product tartaric acid existed.

Fig. 7 shows the spectra of ^1H NMR of ESA, APEM, and PEM in $(\text{CD}_3)_2\text{SO}$. From the spectrum, we can obtain that peaks around 2.50 ppm are also assigned to the solvent residual peak of $(\text{CD}_3)_2\text{SO}$, 3.327 ppm is attributed to C–H (three-membered ring) in curve (a). The chemical shift in the region from 4 to 6 ppm is assigned to propenyl protons ($\text{CH}_2=\text{CH}-\text{CH}_2-$) in curve (b). There are no peaks in this range and around 3.327 ppm in curve (c), indicating that closed-loop C–O–C absorption peaks of ESA and the double bond absorption peaks of APEM completely disappear. As a result, the free radical polymerization among ESA and APEM has occurred, which is corresponding to the result of FTIR analysis.

3.2. Comparison of inhibitors on inhibiting CaCO_3 scale

The scale inhibition performance of ESA-APEM on calcium carbonate in simulated scale inhibition solutions at different concentrations of inhibitor is shown in Fig. 8. It is clear that inhibition efficiency gradually increases with the increase in the concentration of inhibitors. The maximum efficiency of PEM is as high as 94.5% in the concentration of

12 mg/L. Moreover, ESA-APEM exhibits an obvious threshold effect, namely, after the concentration of the polymer runs up to about 8 mg/L, the inhibition efficiency does not obviously increase with the increasing of concentration of the polymer. It should be noticed that the similar effect of the dosage on the performance behavior has been reported in earlier studies [28,29].

Furthermore, to understand the performance of PEM, the same inhibition experiments were conducted with commercial inhibitors at the identical conditions, such as DTPMP, ATMP, PESA, HPMA, and PAA. As is shown in Fig. 8, ESA-APEM displayed superior control power compared with other inhibitors in preventing the growth of CaCO_3 scale. The inhibition efficiency of PAA and HPMA, only containing the carboxyl groups, is 52.2% and 66% at 18 mg/L. Also, we can find that PESA containing carboxyl and ether groups and possessing similar molecular structure to PEM inhibitor but can hardly control CaCO_3 scale even at a high dosage. These results indicate that the side-chain polyethylene (PEG) segments of APEM play an important role during the control of calcium carbonate scales. Besides, the oxygen atom in the ether and ester groups can adsorb on the surface of calcium carbonate crystal to prevent its growth and are easily biodegradable since the ester bonds can be hydrolyzed into carboxyl and hydroxyl groups [20,30]. Taking Fig. 8 into account, it can conclude that the studied inhibitor PEM is a great nonphosphorus scale inhibitor for CaCO_3 in cooling water systems.

3.3. Comparison of inhibitors on inhibiting CaSO_4 scale

Another common precipitation in cooling water system is calcium sulfate, which has caught much attention of academic and industrial researchers [6]. Scale inhibition performance of the modified scale inhibitor, as well as four commercial ones and PESA, on calcium sulfate precipitation, are plotted in Fig. 9. At a level of 4 mg/L PEM, the inhibition efficiency of CaSO_4 reaches 98.2%, revealing that the modified polymer

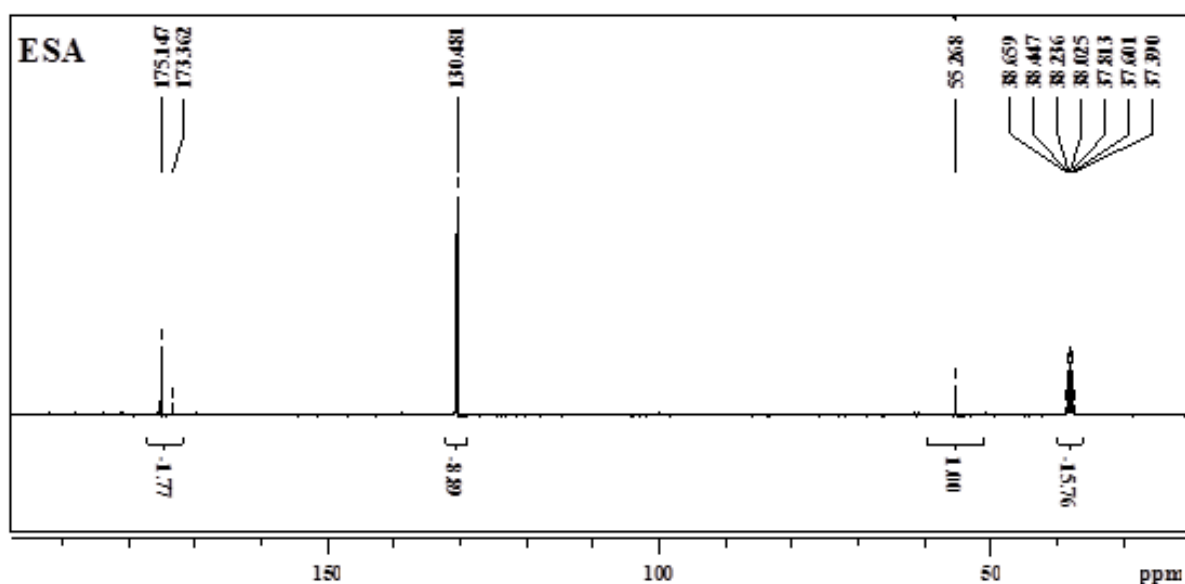


Fig. 6. ^{13}C NMR spectra of ESA.

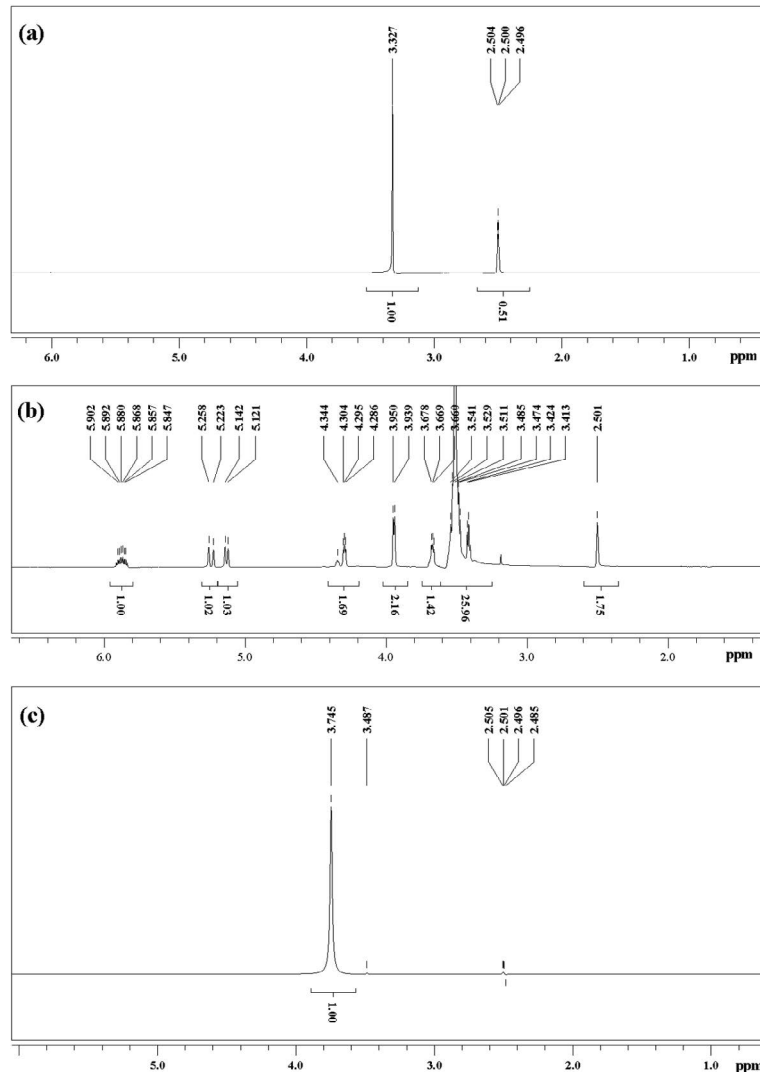


Fig. 7. ¹H NMR spectra of (a) ESA, (b) APEM, and (c) PEM.

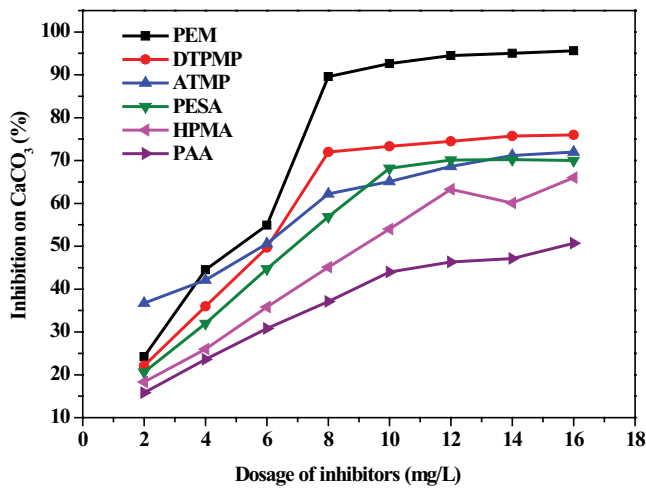


Fig. 8. Scale inhibition of PEM and different commercial inhibitors on CaCO₃ at different concentrations.

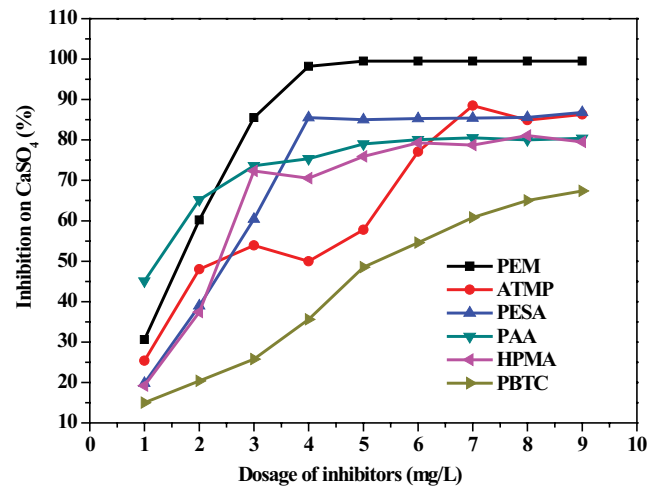


Fig. 9. Scale inhibition of PEM and different commercial inhibitors on CaSO₄ at different concentrations.

PEM is extremely effective for preventing the precipitation of CaSO_4 deposits from aqueous solutions.

Then, compared with raw scale inhibitor PESA and four commercial agents, the product synthesized in our lab demonstrates better performance. The inhibition efficiency increases with the increasing concentration of inhibitors. As displayed in Fig. 9, the capability was as follows: $\text{PEM} > \text{ATMP} > \text{PESA} > \text{PAA} > \text{HPMA} > \text{PBTC}$. The inhibition efficiency of PESA (having similar structure with PEM) can only reach approximately 86.8%; the efficiency of PAA and HPMA (a commonly used polyacrylic acid derivative inhibitor) are 80.4% and 79.5%, respectively; the efficiency of ATMP and PBTC (commonly used phosphorus-containing inhibitors) are about 86.3% and 67.4% with a dosage of 9 mg/L.

3.4. Comparison of inhibitors on inhibiting $\text{Ca}_3(\text{PO}_4)_2$ scale

In addition to its outstanding ability to control calcium carbonate and calcium sulfate scales, PEM also exhibits significant ability to control calcium phosphate scales. As shown in Fig. 10, the ability of modified polymer to control $\text{Ca}_3(\text{PO}_4)_2$ deposits is compared with that of other scale inhibitors. PEM has an efficiency of 99.5% for $\text{Ca}_3(\text{PO}_4)_2$ at a level of 8 mg/L.

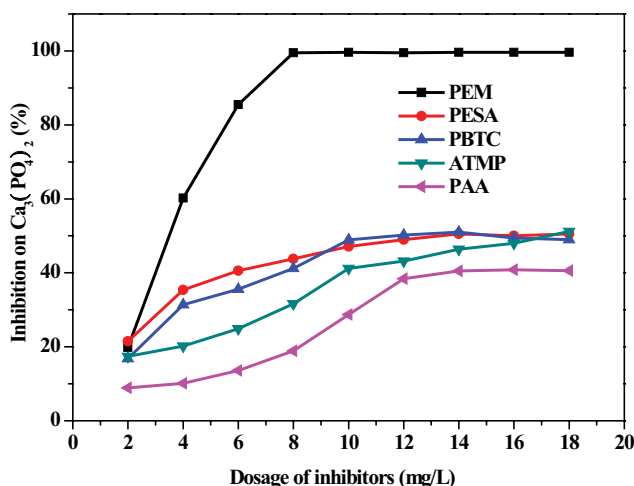


Fig. 10. Scale inhibition of PEM and different commercial inhibitors on $\text{Ca}_3(\text{PO}_4)_2$ at different concentrations.

The inhibitor dosage of PEM strongly affects its performance on calcium phosphate inhibition, and there existed an obvious threshold dosage of 8 mg/L PEM, as is apparent from Fig. 6. When the dosage of PEM was below 8 mg/L, the inhibition on calcium phosphate scales substantially increased when the dosage of PEM increased, while it was not variable with the dosage when it exceeds 8 mg/L.

The data shown in Fig. 10 also indicate that, except for PEM, the other inhibitors investigated display poor calcium phosphate inhibition effect under the same experimental conditions. PEM has superior ability to control $\text{Ca}_3(\text{PO}_4)_2$ deposits, with approximately 100% inhibition at a level of 8 mg/L. However, it is 43.8% for PESA at the same dosage, at which PBTC has only 41.2% calcium phosphate inhibition, 31.6% for ATMP and 18.9% for PAA, which is in accordance with the results of supposed. It is obvious that the capacity of preventing the precipitation of Ca^{2+} from bulk solution is $\text{PEM} > \text{PBTC} > \text{PESA} > \text{ATMP} > \text{PAA}$. Although PESA possesses molecular structure similar to PEM, containing carboxyl and ether groups, it can hardly prevent the precipitation of calcium phosphate even at a high dosage. One reason may be the side chain polyethylene segments of APEM during the process of control calcium phosphate scales.

3.5. Effects of solution pH on calcium scales inhibition

The experiments studied the influencing rules of pH value on the calcium scale inhibition by PEM (ESA:APEM [2:1]). The results are shown in Fig. 11 as follows.

As illustrated from Fig. 11, calcium scales inhibitory power all shows downward trend with the increase of pH values of the solution, indicating that scale inhibition efficiency to CaCO_3 , CaSO_4 , and $\text{Ca}_3(\text{PO}_4)_2$ is influenced greatly by the system acidity. As is well known, the concentration of H^+ decreases with the increase of pH value and the equilibria between H^+ and negative ions (CO_3^{2-} , SO_4^{2-} , PO_4^{3-}) break up, resulting in negative ions becoming excessive. More and more CO_3^{2-} , SO_4^{2-} , and PO_4^{3-} in corresponding solutions will promote calcium scales formation [31].

3.6. SEM and XRD characterization of CaCO_3 scales

SEM is one of the widely used nondestructive surface examination techniques. The change of crystal size and modifications, brought about by the polymer PEM addition, was

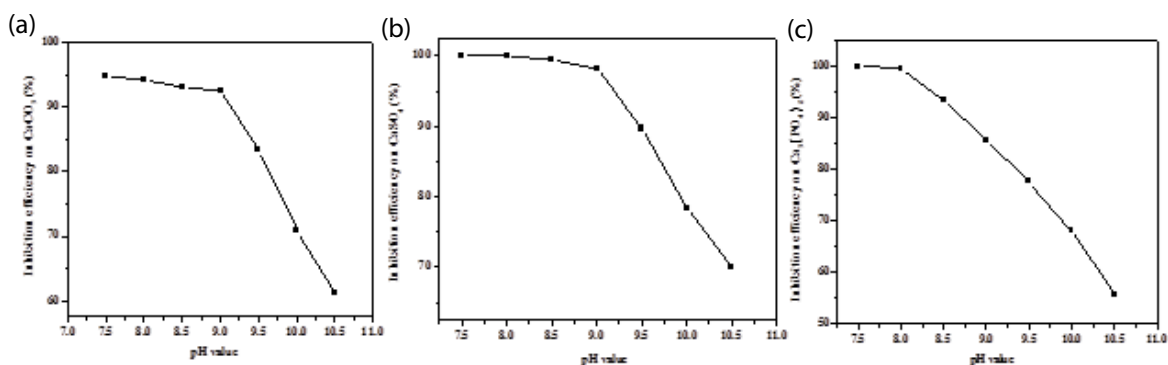


Fig. 11. Influence of pH value on CaCO_3 inhibition of 10 mg/L PEM (a), CaSO_4 inhibition of 4 mg/L PEM (b) and $\text{Ca}_3(\text{PO}_4)_2$ inhibition of 6 mg/L PEM (c).

examined through SEM. The morphology of CaCO_3 crystal in the absence and presence of 8 mg/L polymer is shown in Fig. 12. Fig. 12(a) reveals that calcium carbonate scales are mainly calcite scales, which are symmetry and block-like particles of cubic shape or rhombohedron. Variations in the calcite crystal morphology and the crystal sizes are observed in the presence of the polymer PEM. Fig. 12(b) illustrates that the structure of CaCO_3 crystal appears to be obviously destroyed and there are lots of vaterite phases being more dispersive, which are broken into pieces and set into the bunch crystal. The inhibitor retards the growth of CaCO_3 crystals and distorts the CaCO_3 crystals, leading to poor adhesion to the beaker.

Fig. 13 shows the XRD patterns for the control of CaCO_3 in the polymer system of PEM. In the absence of PEM (Fig. 13(a)), there are strong peaks in the crystal faces of (012), (104), (006), (110), (113), (202), (018), and (116), which are corresponding to calcite phases, the most thermodynamically

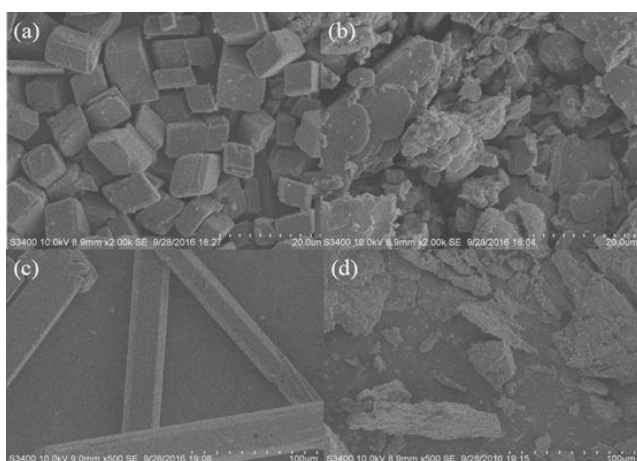


Fig. 12. SEM images of CaCO_3 (a) and (b) and CaSO_4 (c) and (d) scales, (a) without PEM, (b) with 8 mg/L PEM, (c) without PEM, (d) with 4 mg/LPEM.

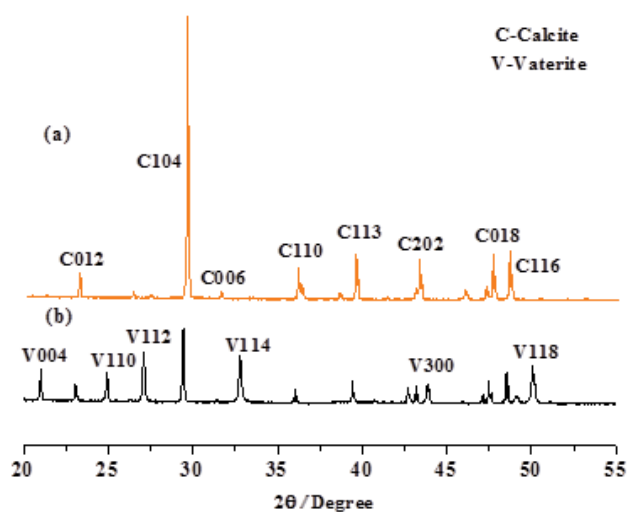


Fig. 13. XRD analysis of CaCO_3 scales (a) without PEM, (b) with 4 mg/L PEM.

stable form of calcium carbonate. With the addition of polymer, the CaCO_3 form changed into vaterite, peaks of (004), (110), (112), (114), (300), and (118), shown in Fig. 13(b). Vaterite is the least stable form of calcium carbonate and easy to disperse in water solution [32].

3.7. SEM characterization of CaSO_4 scales

Figs. 12(c) and (d) show the micro morphology of the CaSO_4 crystal which was obtained directly by filtration from the solution used in static scale inhibition method experiments. It can be seen that the application of the polymer in the system (Fig. 12(d)) is an effective way to control the morphology of the calcium sulfate. As is seen from Fig. 12(c), the obtained crystal samples are looked similar to a slim needle and have smooth surface without scale inhibitor. With the addition of PEM, there are many crystal defects on the surface of samples, which have loose structure with reduced crystallinity. It could be considered that PEM molecules may absorb on the active sites of growing crystal surface and distort the CaSO_4 crystal lattice, so the defects appear on the crystal surface. With the piece form, the deposition will be easily removed from flowing water with enough shear force.

3.8. TEM characterization of $\text{Ca}_3(\text{PO}_4)_2$ scales

In order to analyze the influence of PEM on the growth of calcium phosphate crystal, calcium phosphate scales were collected according to the experimental method on the condition of the appropriate concentration. TEM images of $\text{Ca}_3(\text{PO}_4)_2$ scale particles obtained in the absence and presence of PEM are shown in Fig. 14. Massive bulk-shaped calcium phosphate particles of a size of about 200 nm are obtained without polymer (Fig. 14(a)), while in the addition of 4 mg/L PEM, the calcium phosphate particles become irregular and the size is about 5–100 nm (Fig. 14(b)), indicating that the PEM inhibitor obviously decreased the size of calcium phosphate solid particles thereby dispersing them throughout a fluid.

3.9. Mechanism of scale inhibition

According to the literature, we know that scale deposit formation involves two processes in series: diffusional transport of the crystal forming ions toward the crystallizing deposit and incorporation of the ions on growth sites of the crystal lattice by surface reaction. Fig. 15 displays the second process of scale suppression. Both PESA and PEG (marked with orange ribbons in Fig. 15) segments are hydrophilic blocks and exist randomly in water [33]. Once confronted with Ca^{2+} ions, the $-\text{COOH}$ groups of PEM can recognize and react with the positively charged ions, leading to the spontaneous formation of PEM-Ca complexes (encapsulation zone). In this case, Ca^{2+} is bound with carboxyl groups via excellent chelating ability and powerful affinities. Then, a bedded structure of PEG (outer shell), $-\text{COOH}-\text{Ca}$ complexes (middle layer) and PEG (inner shell) is formed, depicted as chelation process. These chelated compounds are extremely stable toward aqueous phase because of the encapsulated hydrophilic PEG segments. In other words, the inhibition

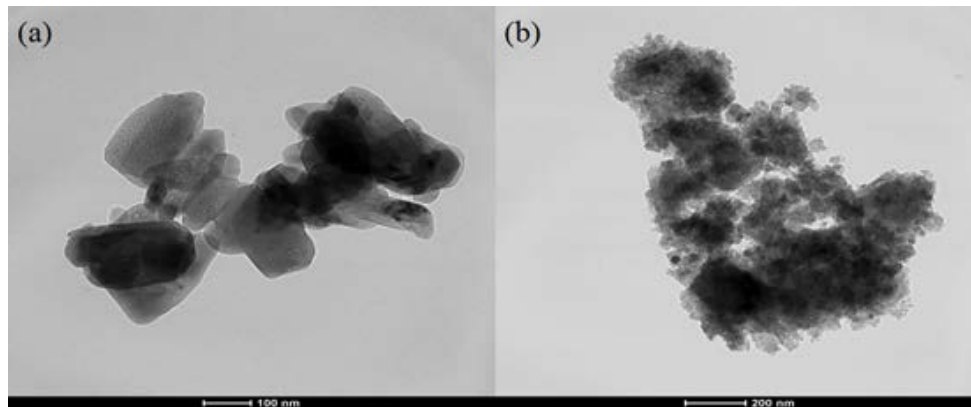


Fig. 14. TEM images of the $\text{Ca}_3(\text{PO}_4)_2$ scale (a) without PEM, (b) with 4 mg/L PEM.

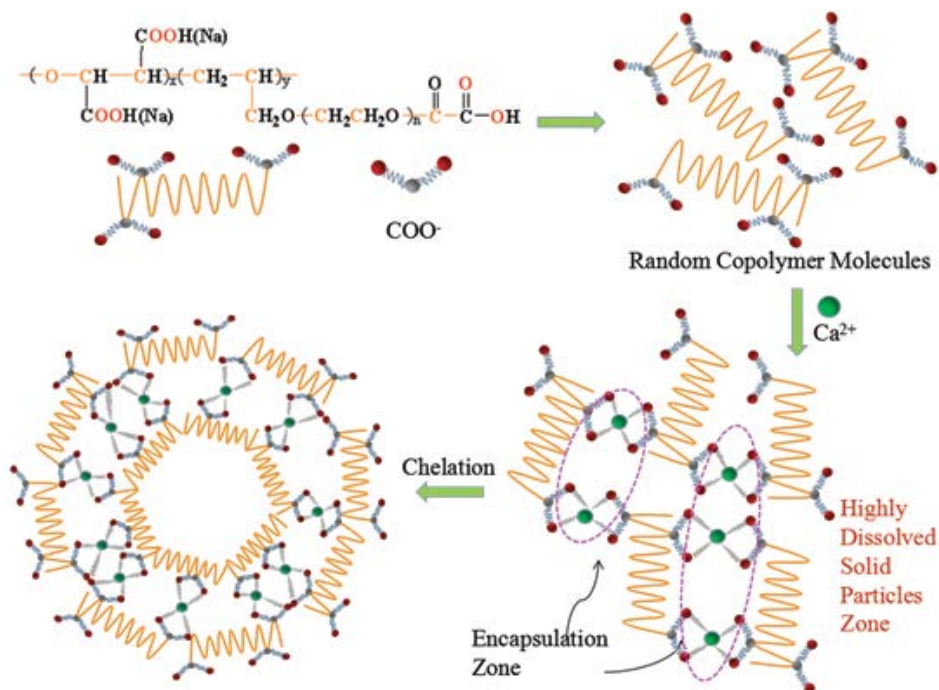


Fig. 15. Schematic illustration of chelation mechanism.

process is involved with adsorption of anti-scalant molecules on active growth sites of the crystallization surface thereby retarding scale growth.

4. Conclusions

In summary, PEM containing carboxylic, hydroxylic, ether and ester groups, a new modified polyepoxysuccinic acid (PESA) scale inhibitor, was successfully synthesized. Compared with the recent commercial inhibitors, DTPMP, PAA, HPMA, PESA, ATMP, and PBTC, PEM possessing PEG showed a superior inhibitory efficiency. The polymer possessed excellent calcium carbonate inhibition, approximately 94.5% at a level of 12 mg/L, along with a superior ability to control calcium sulfate and calcium phosphate scales, that is at a level of 4 mg/L PEM, the inhibition efficiency of CaSO_4

reached 98.2%, while PEM had an efficiency of 99.5% for $\text{Ca}_3(\text{PO}_4)_2$ at a level of 8 mg/L. The inhibition mechanism is proposed that encapsulation or interaction happened between $-\text{COOH}$ and Ca^{2+} and the core-shell structure was formed. SEM, XRD, and TEM studies showed the crystal structures were not much altered but the polymer brought about changes in crystal habits or crystal morphology.

Acknowledgments

This work was supported by Young Teachers' Research Development Fund of Southeast University Chengxian College (z0016, 2019), the National Nature Science Foundation of China (51673040), the Prospective Joint Research Project of Jiangsu Province (BY2016076-01), Scientific Innovation Research Foundation of College Graduate in Jiangsu Province

(KYLX16_0266), and a Project Funded by the Priority Academic Program Development of Jiangsu Higher Education Institutions (PAPD) (1107047002), The Fundamental Research Funds for the Central Universities (2242015k30001), Fund Project for Transformation of Scientific and Technological Achievement of Jiangsu Province of China (BA2016105), based on scientific research SRTP of Southeast University (T16192020), and the Scientific Research Foundation of Graduate School of Southeast University (YBJJ1417).

References

- [1] H.K. Can, G. Üner, Water-soluble anhydride containing alternating copolymers as scale inhibitors, *Desalination*, 355 (2015) 225–232.
- [2] C. Wang, T. Shen, S. Li, X. Wang, Investigation of influence of low phosphorous copolymer antiscalant on calcium sulfate dihydrate crystal morphologies, *Desalination*, 348 (2014) 89–93.
- [3] W.Y. Shi, W. Xu, H. Cang, X.H. Yan, R. Shao, Y.H. Zhang, M.Z. Xia, Design and synthesis of biodegradable antiscalant based on MD simulation of antiscaling mechanism: a case of itaconic acid-epoxysuccinate copolymer, *Z. Comp. Mater. Sci.*, 136 (2017) 118–125.
- [4] S.P. Zhang, H.J. Qu, Z. Yang, C.E. Fu, Z.Q. Tian, W.B. Yang, Scale inhibition performance and mechanism of sulfamic/amino acids modified polyaspartic acid against calcium sulfate, *Desalination*, 419 (2017) 152–159.
- [5] X.H. Li, H. Shemer, D. Hasson, Raphael Semiat, Characterization of the effectiveness of anti-scalants in suppressing scale deposition on a heated surface, *Desalination*, 397 (2016) 38–42.
- [6] D. Hasson, H. Shemer, A. Sher, State of the art of friendly “green” scale control inhibitors- a review article, *Ind. Eng. Chem. Res.*, 50 (2011) 7601–7607.
- [7] D. Liu, W.B. Dong, F.T. Li, F. Hui, J. Lédion, Comparative performance of polyepoxysuccinic acid and polyaspartic acid on scaling inhibition by static and rapid controlled precipitation methods, *Desalination*, 304 (2012) 1–10.
- [8] J.Y. Feng, L.J. Gao, R.Z. Wen, Y.Y. Deng, X.J. Wu, S.L. Deng, Fluorescent polyaspartic acid with an enhanced inhibition performance against calcium phosphate, *Desalination*, 345 (2014) 72–76.
- [9] G. Wei, Y. Xu, R.C. Xiong, A study on biodegradability of scale inhibitors, *J. Beijing. Univ. Chem. Technol.*, 28 (2001) 59–62.
- [10] B. Michael, F.M.D. John, Methods of Controlling Scale Formation in Aqueous Systems, USA patent, 1991, US5062962.
- [11] D.B. Rodney, W.H. Stephen, Ether Hydroxypolycarboxylate Detergency Builders, USA patent, 1987, US4654159.
- [12] W.Y. Shi, C. Ding, J.L. Yan, X.Y. Han, Z.M. Lv, W. Lei, M.Z. Xia, F.Y. Wang, Molecular dynamics simulation for interaction of PESA and acrylic copolymers with calcite crystal surfaces, *Desalination*, 291 (2012) 8–14.
- [13] J.X. Chen, L.H. Xu, J. Han, M. Su, Q. Wu, Synthesis of modified polyaspartic acid and evaluation of its scale inhibition and dispersion capacity, *Desalination*, 358 (2015) 42–48.
- [14] X.H. Zhou, Y.H. Sun, Y.Z. Wang, Inhibition and dispersion of polyepoxysuccinate as a scale inhibitor, *J. Environ. Sci.*, 23 (Supplement) (2011) S159–S161.
- [15] V. Annibaldi, A.D. Rooney, C.B. Breslin, Corrosion protection of copper using polypyrrole electrosynthesised from a salicylate solution, *Corros. Sci.*, 59 (2012) 179–185.
- [16] Y.Z. Zhao, L.L. Jia, K.Y. Liu, P. Gao, H.H. Ge, L.J. Fu, Inhibition of calcium sulfate scale by poly (citric acid), *Desalination*, 392 (2016) 1–7.
- [17] Y. Zhang, H.Q. Yin, Q.S. Zhang, Y.Z. Li, P.J. Yao, Synthesis and characterization of novel polyaspartic acid/urea graft copolymer with acylamino group and its scale inhibition performance, *Desalination*, 395 (2016) 92–98.
- [18] M. Chaussemier, E. Pourmohtasham, D. Gelus, State of art of natural inhibitors of calcium carbonate scaling, *Desalination*, 356 (2015) 47–55.
- [19] A. Zhang, Y.M. Zhou, Q.Z. Yao, T.T. Wang, J. Li, Y.Y. Chen, Q.L. Nan, M.J. Zhang, W.D. Wu, W. Sun, Inhibition of calcium carbonate and sulfate scales by a polyether-based polycarboxylate antiscalant for cooling water systems, *Desal. Wat. Treat.*, 77 (2017) 306–314.
- [20] Y.Y. Chen, Y.M. Zhou, Q.Z. Yao, Y.Y. Bu, H.C. Wang, W.D. Wu, W. Sun, Preparation of a low-phosphorous terpolymer as a scale, corrosion inhibitor, and dispersant for ferric oxide, *J. Appl. Polym. Sci.*, 132 (2015) 1–7.
- [21] GB/T 16632-2008, Determination of Scale Inhibition Performance of Water Treatment Agents – Calcium Carbonate Precipitation Method, China.
- [22] SY/T 5673-1993, Determination of Scale Inhibition Performance for the Design of Industrial Oil Fieldwater Treatments, China.
- [23] GB 50050-95, Code for Design of Industrial Recirculating Cooling Water Treatment, China.
- [24] ISO 6878:2004, Water Quality – Determination of Phosphorus – Ammonium Molybdate Spectrometric Method.
- [25] Z. Liu, Z. F. Liu, X.H. Li, X. Wang, Synthesis, characterization and performance of ESA/AMPS polymer, *Sci. Technol. Eng.*, 8 (2013) 2124–2127 (in Chinese).
- [26] S. Li, J.J. Yang, Y.X. He, T.Y. Song, F. Xiang, Q.Y. Wu, J.N. Zhang, M.Y. Wu, Synthesis and scale inhibition performance of ESA/AMPS polymer, *J. Jishou Univ.*, 36 (2015) 44–48 (in Chinese).
- [27] X. Bai, H.H. Li, L.H. Zhang, Y.L. Zhang, Z.F. Liu, Synthesis, characterization and scale inhibition performance of ESA/AMPS polymer, *J. Hebei Acad. Sci.*, 32 (2015) 54–59 (in Chinese).
- [28] C. Wu, T. Yu, C. Grant, Effect of chelation chemistry of sodium polyaspartate on the dissolution of calcite, *Langmuir*, 18 (2002) 6813–6820.
- [29] N. Tsutsumi, M. Oya, W. Sakai, Biodegradable network polyesters from gluconolactone and citric acid, *Macromolecules*, 37 (2004) 5971–5976.
- [30] Y.Y. Bu, Y.M. Zhou, Q.Z. Yao, Y.Y. Chen, W. Sun, W.D. Wu, Inhibition of calcium carbonate and sulfate scales by a non-phosphorous terpolymer AA-APEY-AMPS, *Desal. Wat. Treat.*, 57 (2016) 1977–1987.
- [31] T.T. Wang, Y.M. Zhou, Q.Z. Yao, J. Li, A. Zhang, Y.Y. Chen, X.N. Chen, Q.L. Nan, M.J. Zhang, W.D. Wu, W. Sun, Synthesis of double-hydrophilic antiscalant and evaluation of its CaCO_3 , CaSO_4 and $\text{Ca}_3(\text{PO}_4)_2$ precipitation performance, *Desal. Wat. Treat.*, 78 (2017) 107–116.
- [32] Y.Y. Chen, Y.M. Zhou, Q.Z. Yao, Y.Y. Bu, H.C. Wang, W.D. Wu, W. Sun, Evaluation of a low-phosphorous terpolymer as calcium scales inhibitor in cooling water, *Desal. Wat. Treat.*, 18 (2015) 945–955.
- [33] G.Q. Liu, M.W. Xue, H. Yang, Polyether copolymer as an environmentally friendly scale and corrosion inhibitor in seawater, *Desalination*, 419 (2017) 133–140.